

Action Anticipation for Collaborative Environments: The Impact of Contextual Information and Uncertainty-Based Prediction

Clebeson Canuto^a, Plinio Moreno^b, Jorge Samatelo^a, Raquel Vassallo^a, José Santos-Victor^b

^aRoom 20, CT-II, Department of Electrical Engineering, Federal University Espírito Santo, Av. Fernando Ferrari, 514, Goiabeiras, 29075-910, Vitória - ES - Brazil

^bFloor 7, North Tower, Institute for Systems and Robotics, Instituto Superior Técnico, Universidade de Lisboa, Av. Rovisco Pais, 1, 1049-001, Lisbon, Portugal

Abstract

For effectively interacting with humans in collaborative environments, machines need to be able to predict (i.e. anticipate) future events, in order to execute actions in a timely manner. However, the observation of the human limbs movements may not be sufficient to anticipate their actions in an unambiguous manner. In this work we consider two additional sources of information (i.e. context) over time, gaze movements and object information, and study how these additional contextual cues improve the action anticipation performance. We address action anticipation as a classification task, where the model takes the available information as the input, and predicts the most likely action. We propose to use the uncertainty about each prediction as an online decision-making criterion for action anticipation. Uncertainty is modeled as a stochastic process applied to a time-based neural network architecture, which improves the conventional class-likelihood (i.e. deterministic) criterion. The main contributions of this paper are three-fold: (i) we propose a deep architecture that outperforms previous results in the action anticipation task, when using the Acticipate collaborative dataset; (ii) we show that contextual information is important to disambiguate the interpretation of similar actions; (iii) we propose the minimization of uncertainty as a more effective criterion for action anticipation, when compared with the maximization of class probability. Our results on the Acticipate dataset showed the importance of contextual information and the uncertainty criterion for action anticipation. We achieve an average accuracy of 98.75% in the anticipation task using only an average of 25% of observations. In addition, considering that a good anticipation model should also perform well in the action recognition task, we achieve an average accuracy of 100% in action recognition on the Acticipate dataset, when the entire observation set is used.

Keywords: Action Anticipation, Context Information, Bayesian Deep Learning, Uncertainty

1. Introduction

Humans have the natural ability to interact with each other and perform joint tasks. Part of this ability is due to their capacity of perceiving the environment and recognizing patterns that help them anticipate the actions of others, and thus make better decisions. Similarly, artificial machines need this capac-

Email addresses: clebeson.canuto@gmail.com (Clebeson Canuto), plinio@isr.tecnico.ulisboa.pt (Plinio Moreno), jorge.samatelo@ufes.br (Jorge Samatelo), raquel@ele.ufes.br (Raquel Vassallo), jasv@isr.tecnico.ulisboa.pt (José Santos-Victor)

ity of anticipating actions, in order to act accordingly and achieve an effective interaction with humans[1].

Action anticipation and action recognition are two different tasks. The “action recognition” task is based on a model that uses an entire sequence of information, which represents one performed action, in order to associate the observed action to one possible action class[2]. If decision-making depends on the entire action, it only can be performed after the action execution. However, this approach is not suitable for systems that manage risks or perform joint tasks with humans. For instance, in a situation where a self-driving car approaches a pedestrian, it must perceive whether the pedestrian will cross the road in time, in order to safely stop or deviate the car if necessary. In this scenario, the model must not only recognize actions but, more importantly, anticipate these actions.

Action anticipation consists of classifying an action even before it occurs, by using the partial information provided up to the a certain moment in time. Usually, an anticipation model is more complex than a recognition one. This comes from its capacity of classifying an action based on an incomplete sequence of data, which makes the choice of the correct class more uncertain. Ideally, every anticipation model should be capable of recognizing actions; on the other hand, not every recognition model will be able to anticipate an action.

In the last few years, deep learning has achieved the state-of-the-art results in many tasks, such as image recognition [3, 4, 5], natural language processing [6, 7] and action/activity recognition [8, 9, 10]. Some works, like [11, 12, 13], represent an action by estimating the movement of the involved actors (i.e. users). In the case of simple and unambiguous actions, the movement can be sufficient for a successful recognition/anticipation task. But in the case of more complex and ambiguous actions, where the information about objects, persons, environment configuration, the movements of actions performed previously, will not be enough to recognize/anticipate actions successfully. Furthermore, some details during action anticipation, such as objects’ position, the relation between hands and object/person and the type of object manipulated, can offer as much or even

more information than only movement. As such, using only movement, the model rules out the context, a critical information that can help characterizing the actions.

Regarding the action recognition task, the two-stream approaches [9, 10, 14] are the most successful ones, because they use movement as the main source of information to describe each action, and they use the context as an additional information that can help characterize each class individually. In these solutions, the movement is the optical flow calculated between sequential images, and the contextual information [15] is extracted in an implicit way by CNNs (Convolutional Neural Networks)[16]. However, to extract the implicit contextual information from images in a self-supervised manner, the training procedure of the CNN models require very big datasets to achieve great results. As consequence, the two-stream approaches are not effective when solving problems provided by small datasets, such those commonly used for human-human or human-robot collaboration.

In this work we focus on context-based action anticipation with small datasets, where instead of implicitly learning the visual context, we define the contextual information in an action anticipation problem. Regarding the Acticipate dataset [1], where one person hands over objects to another one, and receives them back, the dyadic interaction task requires the future prediction (i.e. anticipation) of arm and head motion, gaze and object position. A previous work [17] has shown that using the eye gaze and the 3D pose of the main character in the Acticipate dataset, a time-based deep learning architecture is able to anticipate his actions. As defined in [18], context is any information that can be used to characterize an entity. Therefore, when considering the 3D pose/movement as the entity main source of information that represents an action, the eye gaze in [17] can be seen as context information. Therefore, we extend the number of actions in the Acticipate dataset, considering the new actions *receive* and *pick*, which adds ambiguity into *give* and *place* actions correspondingly. In addition, we consider an additional element of context information, which is the position of the object to be passed. Finally, instead of using

3D pose and gaze as in [17], we use only information taken from RGB images. This makes our proposal more general and less dependent of intrusive and/or expensive sensors.

Even achieving satisfactory results in their experiments, the aforementioned works are not crystal clear about how one could use their solutions in a real-time situation, once they measure the model performance using accuracy or observation ratio. They do not discuss how to handle action anticipation or what kind of function must be used as the decision criterion. In the absence of such discussion, it is unclear how to use this approach in real application, where the data are provided by a stream, such as an RGB camera.

Another problem of most deep learning solutions is their overconfidence in their predictions. A deterministic model will always provide a prediction, even when there is high uncertainty about the correct class, and the final decision becomes very unclear. A trustworthy model should have the ability of assessing its uncertainty about each prediction, to provide to the system the possibility of making more reliable decisions.

Therefore, we propose a context-aware model based on a recurrent neural network with an adaptive threshold. This threshold is calculated via an uncertainty metric, and represents a decision-making criterion for action anticipation. The use of uncertainty greatly contributes to mitigate the problem of overconfidence of a model trained with a small dataset.

In summary, the main contributions of this paper are the following:

- we propose a deep architecture that uses less information than [17], and outperforms the results in action anticipation task using Acticipate dataset. This result holds even in the case of our extended number of actions, which are more ambiguous than the original ones [1].
- we show the importance of context information to disambiguate between similar actions.
- we propose to use the minimization of uncertainty as a more effective decision-making criterion for action anticipation, when compared with the maximization of class probability.

To build a better understanding about the proposal, the next sections will cover, respectively: the related works (Section 2); action anticipation background and related problems (Section 3); the methodology of this work, including the hypotheses raised and its main contributions (Section 4); Bayesian neural networks and uncertainty (Section 5); our proposed approach (Section 6); experiments (Sections 7, results and discussions 8); and finally, conclusions and future works (Section 9).

2. Related Works

In the last few years, due to its importance to perform an effective interaction, action anticipation has been addressed by many researchers [19, 20, 21, 22, 23, 24].

In [22], the authors proposed to decrease the dimensionality on RNNs by allowing sharing of weights, and improve the temporal representation of an action by using an RBF kernel (Radial Base Function) over the hidden-state of an LSTM. They proposed to feed an LSTM with features extracted by a CNN. Next, they applied an RBF over the LSTM hidden states, and lastly, the RBF outcome is given as input to a Multilayer Perceptron (MLP). The authors use between 20% and 50% of a video to predict next features and then performing the anticipation.

In [12], the authors use a convolutional auto-encoder network to predict the next movement of a video. Such movement is generated by a ranking loss function applied over the difference between consecutive images in a sequence, and is stored in a still RGB image called Dynamic Image[25]. With a Markov assumption, after generating a sequence of dynamic images by using S frames for each one, the model generates the next k dynamic images, where $k \geq 1$. Further, those images feed a model that outputs the probability distribution over action classes.

In both works, the authors did not clarify how action anticipation would be performed in a real scenario, where it is not possible to know the size of the sequence. They did not discuss what kind of threshold could be used in such a situation. In complement, a drawback these kind of approaches is their need for big datasets to train their models, once they

use images and models with high capacity. Another drawback is to use movement as only source of information of an action, which can harm actions that are related not only to movement but also to context information.

The above mentioned approaches are not suitable to be applied in small datasets, once the high capacity of their models can lead them to overfitting. Therefore, [17] proposes a different method to anticipate action in the Acticipate dataset - a small collaborative dataset used to understand the role of gaze on action anticipation[1], explained in Section 4. Their approach consist of feeding an LSTM cell with a 3D pose (Motion Capture-MoCap information) and gaze (fixation points), and then pass the LSTM output through a softmax classifier. They trained two models with different observations: one with only 3D pose and another with 3D pose plus eye gaze. As a result, they concluded that the actions in the dataset could be anticipated up to 92ms before when the model uses the gaze as a complement information to the pose. These results helps us see the importance of using more than only movement (in their case, the pose evolution in time) to anticipate actions. However, the authors did not attempt to the fact that their model did not recognize all the actions (100% of action recognition accuracy) even after seeing the whole sequence. Furthermore, their results for action anticipation was shown based only in one action sample. More conclusive results should present statistics for all classes in the entire dataset. In complement, they also did not find the answer to when a model must anticipate an action. From their comments, we assume that it may be done using a threshold on the probability value.

After these explanations, our main objectives in this work are:

- propose a model that improves results in [17] even when using only RGB images;
- present how context can be used in a neural network architecture to improve action anticipation;
- present in detail how to anticipate an action by using a threshold value; and

- propose the use of uncertainty as an effective threshold value that improves action anticipation.

3. Action Anticipation Background

In this section, we describe the definition we adopted for action anticipation, its main properties, and how we address the problem. We can divide the works that try solve anticipation task into two main groups: (i) early action prediction, where an action must be predicted before it is fully executed [26, 23, 27, 28, 29]; and (ii) event anticipation, where an event must be predicted before it starts [30, 31, 31]. In this work, “action anticipation” is understood as in the first set of works: early action prediction by using sequential features.

3.1. Problem Definition

First of all, it is important to define formally the action anticipation task. Let $\mathcal{X} = \{\mathbf{x}_1, \mathbf{x}_2, \dots, \mathbf{x}_n \mid \mathbf{x}_t \in \mathbb{R}^{d \times 1}\}$ be a sequence with N observations that represents the execution of a specific action $y \in \mathcal{Y}$, where \mathcal{Y} is a set with n_a action classes. Here, \mathbf{x}_t represents an observation taken at time t . Now, considering that $\mathcal{X}_{t_1:t_2}$ represents an indexed sequence composed by the observations taken between time t_1 and t_2 , we define a model M for action classification problem as a mapping function parametrized by θ that receives as input $\mathcal{X}_{1:t}$ (t observations from \mathcal{X}) and return as output the vector of probability scores $\mathbf{s} \in [0, 1]^{n_a \times 1}$, representing the probability that sequence \mathcal{X} belongs to each action class.

$$\mathbf{s} = M(\mathcal{X}_{1:t}, \theta). \quad (1)$$

In action recognition tasks, the model M has all the observations of the sequence \mathcal{X} ($t = n$) available to generate the probability score $\hat{\mathbf{s}}$. On the other hand, for action anticipation task, the action is not completely executed, thus only a initial part of \mathcal{X} are available ($t < n$) so that M can infer $\hat{\mathbf{s}}$.

In Equation (1) the parameter θ can be found by solving the following optimization problem:

$$\hat{\theta} = \underset{\theta}{\operatorname{argmax}} \{ \mathcal{L}(\theta, \mathcal{D}) \} \quad (2)$$

where $\mathcal{D} = \{(\mathcal{X}^{(1)}, y^{(1)}), (\mathcal{X}^{(2)}, y^{(2)}), \dots, (\mathcal{X}^{(k)}, y^{(k)})\}$ is the training set, with each pair $(\mathcal{X}^{(i)}, y^{(i)})$ representing an action sequence and its respective label, K is the number of sequences in the training set, and \mathcal{L} is a loss function.

During the prediction time, it is not possible (or at least, not desirable) to know the value of n , and it is thus not possible to know when will the action end. Therefore, at each time t , M uses the observed sequence until the time t ($\mathcal{X}_{1:t}$) and a function g is in charge of predicting the action class at instant t .

$$\begin{aligned}\hat{\mathbf{s}} &= M(\mathcal{X}_{1:t}, \hat{\boldsymbol{\theta}}) \\ \hat{y} &= g(\hat{\mathbf{s}}).\end{aligned}\quad (3)$$

For action recognition tasks, the discriminant function g can be defined as:

$$g(\hat{\mathbf{s}}) = \operatorname{argmax}(\hat{\mathbf{s}}), \quad (4)$$

because the model M is more confident about the probability score assigned to $\hat{\mathbf{s}}$. On the other hand, for action anticipation tasks, since M uses only part of observations, when the distribution $\hat{\mathbf{s}}$ is close to a uniform distribution, it is not possible to be certain about the correct class. Hence, Equation (4) is not an adequate discriminant function to anticipate actions.

In this way, a better option is to use a discriminant function with a threshold parameter p , as presented in Equation (5).

$$g(\hat{\mathbf{s}}, p) = \begin{cases} \operatorname{argmax}(\hat{\mathbf{s}}), & h(\hat{\mathbf{s}}) > p \\ -1, & \text{otherwise} \end{cases}. \quad (5)$$

Once p is specified as a probability value, h can be defined as:

$$h(\hat{\mathbf{s}}) = \max(\hat{\mathbf{s}}) \quad (6)$$

In Equation (5), a value of $p \geq 0.9$ means that the model is certain about its predictions and an action can be anticipated, which favors the use of such model in real-time. On the other hand, when it returns -1 means that it is not certain about the correct class and it needs more observation in order to improve its certainty.

3.1.1. Stochastic models

Stochastic models has the capacity of providing their uncertainty about their predictions. Therefore, when using a stochastic model to anticipate action, a different discriminant function g must be used, such as that presented in Equation (7), where u is an uncertainty value and h is the function that measures the model's uncertainty about its prediction $\hat{\mathbf{s}}$.

$$g(\hat{\mathbf{s}}, u) = \begin{cases} \operatorname{argmax}(\hat{\mathbf{s}}), & h(\hat{\mathbf{s}}) < u \\ -1, & \text{otherwise} \end{cases} \quad (7)$$

There are different types of uncertainties so that, for different models and different proposals, h can assume different forms. In Section 5 we give more details about uncertainty and stochastic models, and, in Section 6, we provide a candidate function for h .

3.2. Evaluation metrics

After determining how to anticipate an action, it is essential to decide how one can ascertain the quality of the model M . Therefore, three measurements are described below.

Accuracy at each observation ratio. Considering that each sequence \mathcal{X} can have a different length N , this metric helps evaluate all sequences in a normalized time scale. Thereby, the success ratio when anticipating an action after a observation ratio r , with an anticipation threshold p , can be calculated as follows:

$$ACC(r) = \frac{1}{K} \sum_{i=1}^K \operatorname{pred}(\mathcal{X}_{1:\lceil r \times N \rceil}^{(i)}, y^{(i)}, p), \quad (8)$$

where,

$$\operatorname{pred}(\mathcal{X}_{1:t}, y, p) = \begin{cases} 1, & g(M(\mathcal{X}_{1:t}), p) = y \\ 0, & \text{otherwise} \end{cases}. \quad (9)$$

In Equation (8), in terms of r , $t = \lceil r \times N \rceil \forall r \in (0, 1]$, where N is number of observation in a sequence $\mathcal{X}^{(i)}$. However, in terms of t , $r = t/N \forall t \in \{1, 2, \dots, N\}$.

Accuracy of anticipated actions. This classification metric measures the success ratio of the model M when anticipating actions. It is calculated as the

average accuracy of each classification. Therefore, when using this metric, we are not regarding in which observation the action was predicted but whether it was predicted correctly or not. Algorithm 1 presents how it is calculated.

```

Result: ant_acc
data ← load_dataset()
num_actions ← get_size(data)
p ← threshold_value
M ← load_model()
corrects ← 0
for k=1 to k=num_actions do
  | X ← data[k]
  | y ← get_label(X)
  | N ← get_size(X)
  | for t=1 to t=N do
  | | pred ← g(M(X[1 : t]), p) if pred ≥ 0
  | |   then
  | | | if pred = y then
  | | | | corrects ++
  | | | end
  | | | break
  | | end
  | end
end
ant_acc ← corrects/num_actions

```

Algorithm 1: Calculation of anticipation accuracy for an action anticipation model.

Expected observation ratio. This measurement focuses on the expected amount of observations necessary to anticipate correctly an action. It can be implemented according to Equation (10). Note that when the model is correct, it receives the value t , which corresponding to the observation where the prediction is executed. However when it misses the anticipation, it is penalized by receiving the sequence size N .

$$E_{obs} = \frac{1}{K} \sum_{i=1}^K obs(\mathcal{X}^{(i)}, y^{(i)}, p), \quad (10)$$

where,

$$obs(\mathcal{X}, y, p) = \frac{1}{N} \min(\{f_{pred}(\mathcal{X}_{1:t}, y, p, t, N)\}_{t=1}^N)$$

$$f_{pred}(\mathcal{X}_{1:t}, y, p, t, N) = \begin{cases} t, & pred(\mathcal{X}_{1:t}, y, p) = 1 \\ N, & \text{otherwise} \end{cases}.$$

4. Methodology

For a better understanding of how our intuitions have arisen and resulted in our proposal, it is necessary to analyze the used dataset and thus realize how the questions came up.

4.1. Acticipate dataset

The Acticipate dataset¹ was acquired with the proposal of studying the influence of gaze in action and/or intention anticipation [1, 17] in a collaborative environment. It comprises 120 trials, distributed into six classes. During the acquisition, the actor was wearing an eye gaze tracker binocular glasses (Pupil Labs eye-tracker [32]) and a suit with 25 markers. He should perform six different actions: give an object (left, middle, or right) and place an object (right, middle, or left). In the *give* actions, he should give an object (in this case, a small red ball) to one of the three volunteers located on: his right side, left side, or in front of him (middle). In the *place* actions, he should place the same object in one of the three points on the table located at his right, middle (in front of him) or his left. Every action starts with the object placed in a point near to the actor and finishes when the object returns to the same point. Figure 1 presents a sample of each action and the object starting point.

Each trial consists of 3 dimensional data corresponding to the positions of the markers on the actor’s suit, captured by an OptiTrack² MoCap system, at 120Hz; 2D gaze fixation point captured by the eye tracker glasses at 60Hz; and an RGB video captured by a camera facing the actor, at 30Hz. The dataset is

¹Download: <http://vislab.isr.ist.utl.pt/datasets/>
²<https://optitrack.com/>

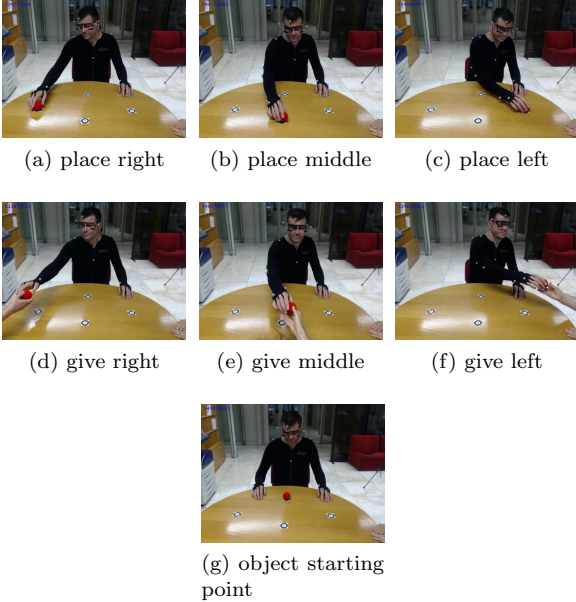


Figure 1: Sample of each action in Acticipate Dataset and the object starting point

unbalanced, because every class has a different number of samples: 17 (place right), 23 (place middle), 20 (place left), 24 (give right), 19 (give middle) and 17 (give left).

In this work, when referring to Acticipate dataset, we call movement the change of position of both arms.

4.2. Dataset Analysis

By analyzing the dataset, it is possible to notice that, in many cases, the movement has not enough information about action to provide good anticipation. For instance, each action of *place* and *give* has similar movements depending on its direction (left, middle or right). However, after taking into account gaze information, one can notice that the action can be anticipated long before. Gaze indicates whether the user will place the object on the table or give it to a volunteer. As discussed before, if we take the movement as the principal entity of each action, we can consider gaze as a context information (additional information that helps characterize the entity). Now,

gaze and movement provide enough data to anticipate actions in this dataset. However, if the dataset was divided into more actions, would the gaze be a sufficient source of information to anticipate them?

An interesting but not considered characteristic of this dataset is that, once the interaction involves only one object, after performing each action, the actor must place the object at its starting point. Thus, when he places the object, he must *pick* it up, and when he gives the object to someone, he must *receive* it back. A simple example of this behavior can be seen in Figure 2. In that way, we can extend the dataset from 6 actions to 12 actions: *give*, *place*, *pick* and *receive* (each one with the directions left, right and middle).



(a) Place middle



(b) Give right

Figure 2: Sample of two actions (place middle and give right) from Acticipate Dataset

Considering now the extended dataset, if we constrain the analyses to the movement and gaze (Figure 3 (a-d)), we notice that, even with gaze, it is not possible to perform right anticipation between actions *give/receive* or *place/pick* when they are toward the same direction. In this case, it is necessary to wait for more observations.

On the other hand, when applying no constraint on what we can analyze in each image (Figure 3 (e-h)), we can anticipate actions of the extended dataset as fast as in its original configuration. In some cases, as in Figure 3 (f), the action can be anticipated after

observing the first frame. This is possible because we take object information into account as another essential context information. For instance, the starting position of the object makes possible to anticipate a *pick* action after observing only one image.

Something similar occurs with *receive* actions, where the object is usually out of the scene, being held by a volunteer. For such actions, after seeing the first frame, it is not possible assure which is the action, once it depends on the direction. However, we can tell that it will be a *receive* action. Therefore, the correct anticipation comes after perceiving the gaze or the movement direction. This helps us to eliminate less likely actions and allows us to focus on information that helps finding the right action. Figure 3 illustrates four situations where there are great ambiguities between actions, and the object information is critical to reduce it.

4.3. Anticipation

Although we are able of anticipating actions in the extended dataset, in some cases, there are issues about the anticipation that must be taken into account. Even people can be fooled by their overconfidence in their prediction capacity. In a particular case, as presented in Figure 4, the volunteer wrongly anticipated an action after observing a movement similar to another one. Her confidence in her prediction deceived her. Thus, even people, in some situations, need to be more sure about the action before making a decision. If a person can be fooled by his/her overconfidence, this problem is possibly bigger in a computational model.

The overconfidence about a prediction could lead the model to make wrong decisions in a real-time environment. A possible solution to mitigate such a problem is to provide the model with the ability to estimate the uncertainty about its prediction. In a deterministic model, even with a high value of probability threshold $p > 0.9$, it would anticipate an action when it was overconfident about its prediction. This overconfidence in prediction can be provoked by a lack of data to prevent the model from ambiguous classes.

Thus, a possible solution to increase the model certainty is lead it to make more z prediction before

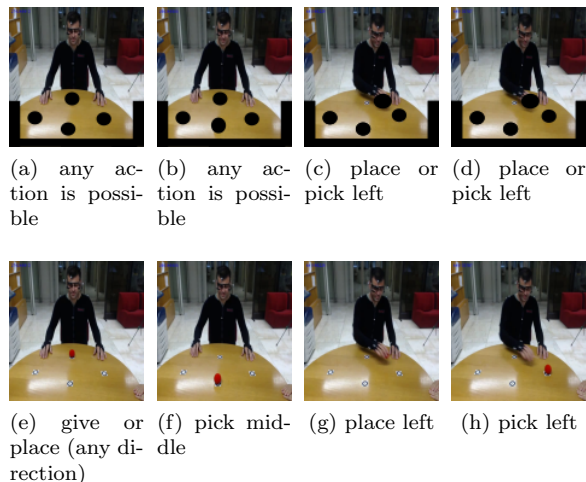


Figure 3: Situations in the extended dataset with great ambiguities when analyzing only gaze and movement. In (a) and (b) any action is possible. It is necessary to wait for the movement to infer the direction but, even after knowing the direction, it is necessary to observe almost the complete action in order to distinguish between the actions *give/receive* and *place/pick*. For both cases in (c) and (d), the movement starts toward the left side, meanwhile the gaze is directed to table. Therefore, the possible action is a *place* or *pick* toward the left direction. For the actions shown in (e)-(h), because the object position is taken into account, the ambiguities can be reduced or even eliminated. In (e) and (f), the number of possible actions are reduced after knowing the object position. In (e), *pick* and *receive* actions are not possible. On the other hand, in (f) only the action *pick middle* is possible. The same occurs in (g) and (h). In (g) the most likely action is *place left* and in (h) the only possibility is *pick left*. Notice that in (f) and (h) the action is anticipated after observing only one image.

making the decision about the correct action class. In this way, if the predicted class remains for the next z observations, the model can be more confident about the correct class and can anticipate the action. However, even though it looks like a good solution, what is the best size for z ? An inaccurate choice of this new parameter can postpone in z observations the anticipation of actions that have no ambiguity problem. In addition, z may not be enough for actions with more ambiguities.

A better solution is to use the uncertainty value in a threshold function rather than probability. Thus, the model can anticipate an action when it is more

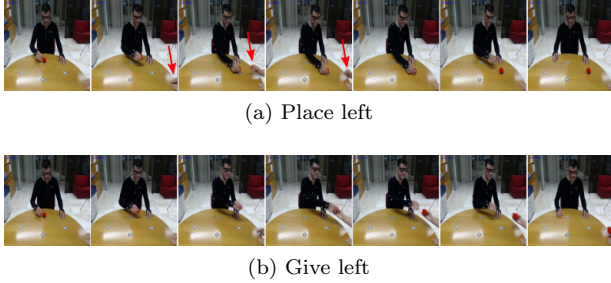


Figure 4: Two action samples from the Acticipate dataset. In (a), the volunteer wrongly anticipated the action, thinking it would be a give left action (shown in (b)) instead of a place left.

certain about its prediction. Therefore, ambiguous actions, which likely provide more uncertainty to the model, would need more observations to be anticipated properly. Once that, those with less ambiguities could be anticipated previously. This solution can be taken as tailored z value for each action chosen by the model during training.

4.4. Hypotheses and contributions

These observations lead us to raise three main hypotheses regarding the Acticipate dataset:

1. more actions generate more ambiguities.
2. context information helps to distinguish different actions represented by similar movements.
3. uncertainty is a more reliable an effective threshold to anticipate action than probabilities are.

In this work the gaze and the object represents the context of each action. So, we propose a model based on Artificial Neural Networks (ANNs) that anticipates actions represented by sequences of that data with varying length. The proposed model has two versions: a deterministic and a stochastic one.

We firstly apply the model to the original dataset with six actions and compare the results with the baseline [17]. Next, the model with the best result becomes the new baseline for three different types of stochastic models. With this approach, we are able to discuss which model is better for action anticipation and their main advantages and drawbacks. The objective of training different model

types with different versions of the dataset is to provide results that lead us to more concise conclusions.

5. Bayesian Neural Networks and Uncertainty

Deep neural networks are usually trained by optimization algorithms based on Stochastic Gradient Descent (SGD). As SGD uses the gradient of the weights, it needs all weights to be differentiable with respect to the loss function. Which implies the weights must be deterministic variables. Therefore, in consequence, most deep neural network models are deterministic, and, for this reason, they are unable to provide their uncertainty about their predictions. Thus, in order to measure uncertainty in this type of models, we must create a Bayesian Neural Network (BNN).

In a Bayesian model a posterior distribution must be inferred by applying the Bayes rule:

$$p(\boldsymbol{\theta}|\mathcal{D}) = \frac{p(\mathcal{D}|\boldsymbol{\theta})p(\boldsymbol{\theta})}{\int p(\mathcal{D}|\boldsymbol{\theta})p(\boldsymbol{\theta})d\boldsymbol{\theta}}, \quad (11)$$

where $p(\boldsymbol{\theta}|\mathcal{D})$ is the posterior distribution over $\boldsymbol{\theta}$ after observing data \mathcal{D} ; $p(\mathcal{D}|\boldsymbol{\theta})$ is the likelihood of \mathcal{D} ; $p(\boldsymbol{\theta})$ is the prior belief about the distribution of $\boldsymbol{\theta}$; and $\int p(\mathcal{D}|\boldsymbol{\theta})p(\boldsymbol{\theta})d\boldsymbol{\theta}$ is the the normalization term (a.k.a evidence or marginal likelihood).

In many cases, the evidence term in Equation (11) turns the posterior inference intractable. However, some works attempted to solve this problem via Variational Inference (VI) [33]. In 2011, [34] proposed in detail how to use VI in Bayesian Neural Networks so that its posterior distribution could be approximated by a Gaussian distribution with known parameters. Although effective, VI was not yet an easy task to accomplish. Therefore, in 2013, [35] proposed a way to train a BNN with VI thought a technique called reparametrization trick, which consists of drawing the activation D of a layer l from a standard Gaussian distribution.

In this sense, the layer l outputs two values, μ and σ , which represents respectively the mean and variance of a Gaussian distribution $N(\mu, \sigma)$. Next, the activation of l is drawn from $D \sim N(\mu, \sigma)$. Aiming

to approximate D by a standard Gaussian distribution ($N(0, 1)$), the authors use variational inference. However, as D is now stochastic, SGD algorithms can not be used in order to train the parameters of l . To solve this problem, they proposed to parametrize D so that μ and σ being deterministic with respect to D , and, by consequence, differentiable with respect to a cost function. In that way, a SGD algorithm can be used to train the parameters of layer l . Equation (12) presents this approach, so-called reparametrization trick.

$$\begin{aligned} D &\sim N(\mu, \sigma) \\ D &= \mu + \sigma\epsilon \end{aligned} \quad (12)$$

Here, the noise ϵ is responsible for the stochasticity in D .

Even with a significant contribution, the authors in [35] used D as the last layer of an encoder, not in all network activations or weights. Hence, in 2015, [36] proposed to use this approach to create a BNN considering every model weight as a distribution instead of a deterministic variable. The reparametrization trick allowed them to use the backpropagation algorithm to train the model via SGD, and to use VI to approximate the factorized weight posterior distribution to a distribution with known parameters. This approach is called Bayes By BackProp (BBB).

Other approaches, as MC dropout[37] and Variational dropout[38], use dropout to obtain an approximation of a Bayesian model.

In MC dropout, the model must have a dropout function before each weight layer. Thus, the Bayesian approximation is achieved by randomly deactivating weights based on a Bernoulli distribution with the probability of $1 - p$, where p is a hyper-parameter. The name MC dropout is given once the model prediction is calculated by the average of S Monte Carlo (MC) samples on the model with the dropout enabled. This process is presented in Equation (17).

Variational Dropout uses the local reparametrization and VI to train and to approximate the neural network model of Bayesian model. With the reparametrization trick in BBB (Equation (12)), after a layer i receiving \mathbf{x}_i as input, it first sample the weights θ from a Gaussian distribution $N(\mu, \sigma^2)$ and

then computes the activation $\hat{y} = \theta^T \mathbf{x}$ as the inner product between \mathbf{x} and θ . On the other hand, in local reparametrization, the activations are sampled directly from a Gaussian distribution, as shown in Equation (13).

$$\begin{aligned} \mu &= \theta^T \mathbf{x} \\ \sigma &= (\theta^2)^T \mathbf{x}^2 \\ \hat{y}_i &= N(\mu, \sigma^2), \end{aligned} \quad (13)$$

Here, $\mathbf{a}^2 = \mathbf{a} \circ \mathbf{a}$, where \circ represents a pointwise (Hadamard) multiplication between \mathbf{a} and \mathbf{a} .

This local reparametrization technique can be used in conjunction with a noise $\xi \sim N(1, \alpha)$ in order to get the posterior $p(\omega|D) = N(\theta, \alpha\theta^2)$, where ω is the variational parameter, θ is the model weight and $\alpha = p/(1-p)$. Equation (14) presents the variational dropout approach.

$$\hat{y} = \theta^T (\mathbf{x} \circ \xi) \quad (14)$$

As ξ is drawn from a Gaussian distribution, the marginal distribution $\hat{y} = p(\hat{y}|\mathbf{x})$ is also a Gaussian distribution. Thus, one can sample \hat{y} directly from its marginal distribution $p(\hat{y}|\mathbf{x})$, as presented in Equation (15).

$$\begin{aligned} \hat{y} &= N(\mu, \sigma^2) \\ \mu &= \theta^T \mathbf{x} \\ \sigma &= \alpha(\theta^2)^T \mathbf{x}^2 \end{aligned} \quad (15)$$

Even though p in MC dropout is a hyperparameter, α in variational dropout can be taken as a trained parameters, giving different importance for each element in $(\theta^2)^T \mathbf{x}^2$.

In a Bayesian model, regardless the approach employed to infer the posterior distribution, the prediction of an observation \mathbf{x}^* is calculated by integrating the likelihood of \mathbf{x}^* over all posterior distribution (Equation (16)). As this process involves an intractable integration, an unbiased approximation can be obtained by a Monte Carlo simulation, as presented in Equation (17).

$$p(y^*|\mathbf{x}^*; \theta) = \int p(D|\theta)p(\theta|D)d\theta \quad (16)$$

$$p(y^*|\mathbf{x}^*; \theta) \approx \frac{1}{S} \sum_{s=1}^S p(y|\mathbf{x}^*; \theta_s) \quad (17)$$

Here, S is the number of samples, y^* is the probability distribution of classes given \mathbf{x}^* , and $\theta_s \sim p(\theta|D)$ is the s^{th} parameter θ drawn from the posterior $p(\theta|D)$. For the variational dropout model, this posterior is $p(\omega|D)$. However, for MC dropout, this posterior distribution is represented by the dropout function inside each network layer.

5.0.1. Uncertainty

There are two main types of uncertainty in Bayesian modeling: aleatoric and epistemic. Aleatoric is the uncertainty of an event (a.k.a irreducible uncertainty). In a classification problem, this uncertainty is related to the event that generates the data. Therefore, even though some works propose ways to assess the aleatory uncertainty of a model [39, 40], it is not an easy task to perform, once in most cases, one can not know how the data was sampled or which event generate them.

Epistemic uncertainty, differently from the aleatoric one, assesses the model uncertainty about the data, and can be easily calculated when the model is stochastic. This type of uncertainty can be decreased by observing more data. Thus, it is important when one wants to know which class needs more data to improve model prediction. A detailed explanation about uncertainties for Bayesian Deep Neural Networks is given in [41].

In this work, we are interested in determining the uncertainty of the model about its prediction, which corresponds to its epistemic uncertainty. In this sense, the more data it receives during training, the more confident it would be about its predictions. Thereby, actions with fewer samples data would lead the model to uncertain predictions. In this case, it is possible to use epistemic uncertainty to realize when the model should wait for more observations to increase its certainty about prediction, and then anticipate the action correctly.

The epistemic uncertainty of a Bayesian neural network model can be estimated by the entropy or the mutual information metrics[41]. In case of a MC simulation with S samples, a model with C actions can calculate the entropy of theses predictions (samples) by using Equation (19) and the mutual information

by Equation (20).

$$\mathbb{E}_{pred}(x, c) = \frac{1}{S} \sum_{s=1}^S p(y = c|x; \theta_s) \quad (18)$$

$$\mathbb{H}(x) = - \sum_{c=1}^C \mathbb{E}_{pred}(x, c) \log(\mathbb{E}_{pred}(x, c)) \quad (19)$$

$$\mathbb{I}(x) = \mathbb{H}(x) + \frac{1}{S} \sum_{c=1}^C \sum_{t=1}^S p(y = c|x; \theta_s) \log p(y = c|x; \theta_s) \quad (20)$$

6. Proposal

In this section, we present our proposed architecture, which is divided into three main steps: feature extraction and selection, feature embedding, and classification model. Next topics will cover each step in detail.

6.1. Feature extraction and selection

This work proposes to use gaze and object information as the context info, and the evolution of the 2D body joints features as the movement information in order to perform action anticipation. Our approach aims to use only RGB images, where gaze and skeleton joints information are not straight available.

Therefore, to obtain gaze and skeleton joints of the people present in the images, we considered to use the Openpose model[42] over each RGB images to extract such information. We used the Openpose version trained for COCO dataset that provides 19 2D joints for the body and 25 2D points for each hand.

Is important to mention that, in [17], the authors used gaze and 3D body joints, since they had glasses and a MoCap system, while, in our approach, we have only 2d joints to use as data, because we are considering just RGB images. Also, because the actor wore glasses during data acquisition, algorithms for 2d gaze estimation did not work. For this reason, we decided to use the head joints as information that likely may represent head direction or even gaze.

However, this representation is a task to be assumed by the model. Aiming to reduce dimensionality, we calculated the central point of each hand instead of using directly their 25 2D points.

For the object information, we extracted the central point of the red ball for each frame by using a segmentation function. All this pre-processing procedure is summarized in Figure 5 and described as follows:

1. Openpose model receives an RGB image representing an observation. This operation results in 19 joints and 25 hand points from each user present in the image.
2. A filter to remove false-positive users is applied.
3. Select the most important joints (arms, shoulders, and head)
4. Use hand points to calculate the central point of each hand
5. Give the same RGB image as input to segmentation function in order to extract the central point of the object.

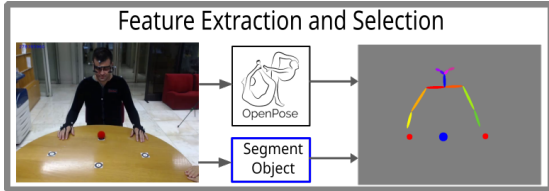


Figure 5: Summary of the feature extraction and selection step.

6.2. Feature Embedding

After the pre-processing step, head information is represented by five 2D points ($V_h \in \mathbb{R}^{10 \times 1}$); object information by one 2D point ($V_o \in \mathbb{R}^{2 \times 1}$); and user pose (movement) by nine 2D points ($V_m \in \mathbb{R}^{18 \times 1}$), where the first seven points represent arms and shoulders, and the last two points represent the hands. Notice that, movement, head, and object have different number of points, which generate an unbalanced feature vector. Because of that the model may consider the movement more important than the other

features. Therefore, we propose to balance the input source by using an embedding structure, in such a way that movement and context features have the same dimension. Besides that, to represent the context, head and object features were also defined with the same dimension, so they had the same importance. The embedding processes is explained below.

1. Embed object information V_o : $E_o = W_o^T V_o$, where $E_o \in \mathbb{R}^{16 \times 1}$ and $W_o \in \mathbb{R}^{2 \times 16}$.
2. Embed head information V_h : $E_h = W_h^T V_h$, where $E_h \in \mathbb{R}^{16 \times 1}$ and $W_h \in \mathbb{R}^{10 \times 16}$.
3. Embed movement information V_m : $E_m = W_m^T V_m$, where $E_m \in \mathbb{R}^{16 \times 1}$ and $W_m \in \mathbb{R}^{18 \times 16}$.
4. Embed context information (E_o, E_h): $E_c = W_c^T (E_o \frown E_h)$, where $E_c \in \mathbb{R}^{1 \times 16}$, $W_c \in \mathbb{R}^{32 \times 16}$ and \frown is a concatenation operator.
5. Create the embedded input vector: $E_{cm} = E_c \frown E_m$, where $E_{cm} \in \mathbb{R}^{32 \times 1}$ and \frown is a concatenation operator.

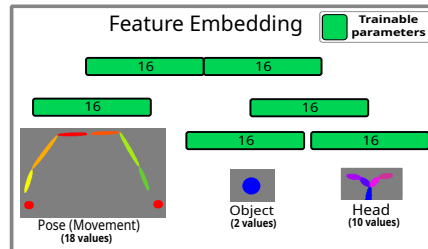


Figure 6: Feature embedding process for each observation. The connections between joints as well as the object shape are showed just for the sake of visualization. However, only their points are used.

Each W_* represents weights that are trained by the model. Thus, during the training phase, the model simultaneously learns to incorporate observations and classify actions.

6.3. Classification model

As the data samples have a sequential nature, the model must take into account the relation between features of different instants. Models as HMM (Hidden Markov Model) and CRF (Conditional Random

Fields) are possible candidates. However, these models assume the Markovian condition: a given observation depends only on the previous one. This assumption might not capture long dependencies on a sequence, which occurs during action execution. Therefore, we decided to use LSTM (Long-Short Term Memory)[43], a variant of RNN that can capture long dependencies in a sequence of observations.

An LSTM contains four trainable gates. These gates are responsible for capturing long and short dependencies in a sequence. An LSTM cell receives as input an observation vector, a hidden state, and an echo cell. The input vector represents the actual observation; the hidden state represents the short-term memory and chooses what information should be paid attention in the next observation. The echo cell represents the long-term memory. At each new observation, the echo cell stores important pieces of information about the actual observation and forget part of its past when it considers less significant. LSTM has been used mainly for NLP [7, 6] but in the last few years recognition tasks in videos are commonly using it as well. The Equations (21)-(26) represent all LSTM gates and activations, respectively:

$$f_t = \sigma_g(W_f x_t + U_f h_{t-1} + b_f) \quad (21)$$

$$i_t = \sigma_g(W_i x_t + U_i h_{t-1} + b_i) \quad (22)$$

$$o_t = \sigma_g(W_o x_t + U_o h_{t-1} + b_o) \quad (23)$$

$$g_t = \Phi(W_o x_t + U_o h_{t-1} + b_o) \quad (24)$$

$$c_t = f_t \circ c_{t-1} + i_t \circ g_t \quad (25)$$

$$h_t = o_t \circ \Phi(c_t) \quad (26)$$

where $\sigma(x)$ and $\Phi(x)$ are, respectively, *sigmoid* and *hyperbolic-tangent* activation functions.

Figure 7 presents the proposed model. It comprises two LSTM cells (layers) followed by a softmax classifier. The first LSTM cell receives as input at time t the embedded input vector $E_{cm}^{(t)}$, the hidden state $h_1^{(t)} \in \mathbb{R}^{1 \times 64}$ and the echo cell $c_1^{(t)} \in \mathbb{R}^{1 \times 64}$. The second LSTM cell receives as input the hidden state $h_1^{(t)}$ resulted from the first layer, the hidden state $h_2^{(t)} \in \mathbb{R}^{1 \times 64}$, and the echo cell $c_2^{(t)} \in \mathbb{R}^{1 \times 64}$. Next, a fully connected layer receives as input $h_2^{(t)}$, applies a transformation using a matrix $W_c f \in \mathbb{R}^{64 \times d}$ (d is the number of actions) and normalize it using a *softmax* function. So, the output of the model is the probability distribution

$$\hat{\mathbf{s}}^{(t)} = p(\hat{y} = a | (E_{cm}^{(t)}, h_1^{(t)}, c_1^{(t)}, h_2^{(t)}, c_2^{(t)}); \theta), \quad (27)$$

where $\hat{\mathbf{s}}^{(t)} \in \mathbb{R}^{1 \times d}$, a represents an action and θ the probabilistic model weights. With this result and choosing a probability threshold value p , by using Equations (5), the anticipation can be performed following the Algorithm 2.

This proposed model is the deterministic version. However, as aforementioned, this work intends to show how the anticipation can be effectively performed by using uncertainty as a threshold. So, three versions of the proposed model will be implemented and tested. A Bayesian LSTM using Bayes By BackProp (BLSTM_{BBB}), an MC dropout Bayesian LSTM based on [44] (BLSTM_{MC}), and a Variational Dropout Bayesian LSTM (BLSTM_{VD}).

The uncertainty is obtained by running the architecture of Figure 7 S times (MC sampling) using the same observation \mathbf{x} (which in the case of Eq. (1)

1. forget gate $f_t \rightarrow$ forget part of the memory stored in the echo cell.
2. input gate $i_t \rightarrow$ select part of the observation to be stored into the next echo cell
3. output cell $o_t \rightarrow$ select what part of the input will be propagated to the next observation by the hidden state.
4. update gate $g_t \rightarrow$ normalize the observation in order to store it into the next echo cell. Part of this information will be forgot by using the input gate.
5. next echo cell $c_t \rightarrow$ forget part of the past observations and store part of the new one.
6. next hidden state $h_t \rightarrow$ select a part of the normalized echo cell by using the output gate.

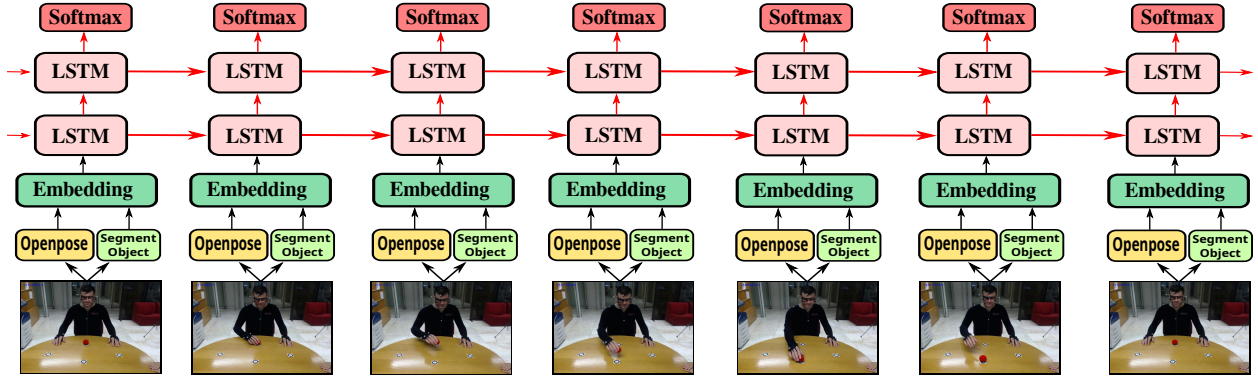


Figure 7: Proposed model architecture

Result: *action*

$action \leftarrow -1$

$p \leftarrow thres_value$

$M \leftarrow load_trained_model()$

$h_1 \leftarrow zeros(1, 64)$

$c_1 \leftarrow zeros(1, 64)$

$h_2 \leftarrow zeros(1, 64)$

$c_2 \leftarrow zeros(1, 64)$

while $action = -1$ **do**

$O \leftarrow get_next_image()$

$F_{cm} \leftarrow extract_features(O)$

$E_{cm} \leftarrow feature_embedding(F_{cm})$

$\hat{Y}, (h_1, c_1, h_2, c_2) \leftarrow M(E_{cm}, (h_1, c_1, h_2, c_2))$

$action \leftarrow g(\hat{Y}, p)$

end

Algorithm 2: Action anticipation algorithm for prediction time in deterministic model.

is a sample \mathbf{x}_t). So, as the model is stochastic, it must give a different value for each prediction. Thus, the Mutual Information (MI) over of the S predictions give us the epistemic model uncertainty about the class prediction for the observation \mathbf{x} . MI can be calculated as presented in Equation (20). This metric was chosen because it takes into account not only entropy between classes (averaged over the S predictions) but also the mean entropy between all of them.

To use mutual information as threshold, Equation (4) must be redefined:

$$g(\hat{\mathbf{s}}^{(t)}, u) = \begin{cases} arg\ max(m(\hat{\mathbf{s}}^{(t)})), & \text{if } h(\hat{\mathbf{s}}^{(t)}) < u \\ -1, & \text{otherwise} \end{cases} \quad (28)$$

where u is an uncertainty value, h is the mutual information function (Equation (20)), and m is the average of the S predictions).

7. Experiments

All experiments in this work use the Acticipate dataset, presented in Section 4. From the dataset, we extracted four different kinds of data by using the procedure described in Section 6: head points, object position, arm joints, and hand position. The head points and object position forms the context; arm joints and hand positions form a pose, which evolution in time represents the movement (also called here main entity). To better compare results and reach more reliable conclusions about how each source of information influences the action anticipation, we decided to carry out experiments using different combinations of the context (head and object) and movement, for the original version of the dataset (6 actions) and its extended version (12 actions). In total, we carried out 11 different experiments. Table 1 presents a summary of these experiments.

The first two experiments (original dataset with 6 actions) provide results that can be compared with

Table 1: List of all experiments

Id	Model	Type	Movement	Context		Dataset Version	
				Head	Object	6 actions	12 actions
1	$DLSTM_{6m}$	Deterministic	✓			✓	
2	$DLSTM_{6mh}$	Deterministic	✓	✓		✓	
3	$DLSTM_{12m}$	Deterministic	✓				✓
4	$DLSTM_{12h}$	Deterministic		✓			✓
5	$DLSTM_{12o}$	Deterministic			✓		✓
6	$DLSTM_{12mh}$	Deterministic	✓	✓			✓
7	$DLSTM_{12mo}$	Deterministic	✓		✓		✓
8	$DLSTM_{12mho}$	Deterministic	✓	✓	✓		✓
9	$BLSTM_{MC}$	MC Dropout	✓	✓	✓		✓
10	$BLSTM_{VD}$	Variational Dropout	✓	✓	✓		✓
11	$BLSTM_{BBB}$	Bayes By BackProp	✓	✓	✓		✓

[17]. Besides, the best one will be taken as the baseline for the next six experiments with the dataset in its extended version. The experiments from 3 to 8 provide results to show the ambiguities between actions and the importance of context to anticipate them. The last three experiments provide results that show the importance of uncertainty in an anticipation model. For this reason, three Bayesian models were implemented: MC dropout, Variational Dropout and Bayes by Backprop. For variational dropout, as mentioned before, we opt to use α (Equation (15)) as a trainable parameter. With these three models we are able to identify which model is best for this kind of application.

7.1. Software and Hardware environments

All models, including Openpose (a deep neural network), were implemented in Pytorch v1.0. Additional parts, as object segmentation, filters and chart plot scripts, were implemented using OpenCV v4.1, Python v3.7, Numpy v1.16.4 and Matplotlib v2.2.3. The computer used in the experiments had the following configuration:

- Linux Operating System, distribution Ubuntu Server 16.04;
- Intel Core i7-7700 processor, 3.60 GHz with 4 physical cores;

- 32 GB of RAM;
- 1 TB of storage unit (hard drive);
- Nvidia Titan V graphic card

7.2. Experiment setups

For each RGB image in the video, was applied the pre-processing procedure described in Section 6. Every missing data related to joints, hands, and the object position was set to -1. Thus, in order to evaluate the model’s quality, each experiment followed a 10-fold cross-validation. The training process was finished when the recognition accuracy (the accuracy achieved at the last frame of the video) in the last five epochs was greater than 99% (early stop) or when the iterations exceeded the maximum number of epochs. We did not use a validation set as early stop condition, because of the small size of the dataset. Dividing the training set into train and validation could harm the result on the test set.

The 11 experiments in Table 1 can be divided into three main categories: deterministic with 6 actions, deterministic with 12 actions and stochastic with 12 actions. In both deterministic experiments, different configurations of the input data (movement, head and object) were achieved by assigning -1 to V_m , V_o , and/or V_h in the entire dataset. For instance, by assigning -1 to V_o , the model considers only movement (V_m) and head (V_h) information. For each one of the

11 experiments proper hyperparameters were used, as presented in Table 2.

8. Results and Discussions

After running all 11 experiments, their results were plotted in many charts (dynamics and statics) and carefully analyzed. Some of these charts are presented and discussed in this section.

8.1. Deterministic models

Figure 8 compares the accuracy at each observation ratio (Equation (8)) for the 2 first experiments ($DLSTM_{6m}$ and $DLSTM_{6mh}$) and the results in [17], all of them carried out on Acticipate dataset with the original 6 actions. Our proposal, even using 2D skeleton joints extracted from images, outperforms [17], that used eye gaze and 3D pose. With *movement + head* information we achieved 80% of accuracy with less than 38% of observations and 90% of accuracy with less than 42%. On the other hand, the authors’ model, in [17], achieves 80% of accuracy after observing more than 43% of information and achieves 90% of accuracy after more than 52% of observations. As discussed before, an effective anticipation model must also be an effective recognizer. Our model $DLSTM_{6mh}$ recognized all actions at the last observation (100% of average accuracy); meanwhile, their model achieved a maximum of 98.37% with a observation ratio 0.63 and decreased to 87% with a observation ratio 1.0. Therefore, besides their model did not recognize all actions in the dataset.

In addition to the results above, $DLSTM_{6mh}$ can anticipate an action 3 frames before than $DLSTM_{6m}$, on average. As the video has a sample rate of 30Hz, this anticipation corresponds to 100ms, which is greater than the 92ms presented in [17] when comparing *pose* with *pose+gaze*. As such, besides outperforming [17], our proposal was able to solve the action recognition problem in the Acticipate dataset and improve the action anticipation results.

Now, by using the extended version of the dataset, the results of the next 6 experiments (from 3 to 8) are presented in Figure 11. They show that $DLSTM_{12m}$, $DLSTM_{12h}$, $DLSTM_{12mh}$ did not achieve 100% accuracy at the last observation. This show that they

were unable to separate actions properly, even when using head information. The new 6 actions are the only difference concerning $DLSTM_{6mh}$ and these three models. As such, when dividing the dataset into more actions, we would generate more ambiguities among them. Then, these results confirm our first hypothesis: more actions generate more ambiguities.

The models that use object information ($DLSTM_{12o}$, $DLSTM_{12mo}$, $DLSTM_{12mho}$), were able to recognize all actions. Further, they achieved better results in the anticipation task. They start with more than 40% of accuracy at the first observation, and the model with complete context ($DLSTM_{12mho}$) achieves 98% of accuracy at the observation ratio of 0.42. Therefore, actions with similar movements can be distinguished better when using the context information. So, This result supports our second hypothesis: context information helps to distinguish different actions represented by similar movements. In addition, we can see how this last model was able to extract relevant information from the object position and head points. Even though the object is represented by only two values (a 2 dimensional point), as we suppose, it provided significant information about the actions to the model. This shows the efficacy of our feature embedding process.

As mentioned above, after using the object information, the model might be able to anticipate some actions after a few number of observations. For better visualization, Figure 10 illustrates the accuracy of the 6 models for the 6 new added actions (receive and pick (left, middle, right)). The models that use object context start with a classification accuracy greater than 65% and achieve 90% of accuracy after less than 10% of observations. The best model reaches 95% of accuracy with less than 5% of observations, on average. In terms of frames, for the Acticipate dataset, that corresponds to an average of 4 frames. These results support our statement about the importance of object information for these 6 new actions.

To measure the anticipation accuracy, we use the Algorithm 2 with threshold $p = 0.9$ for the 6 models. Figure 9 presents the evolution of an action *pick right* after passing throughout the 6 models. The

Table 2: List of hyperparameters used in each experiment

Hyperparameters	Model Configurations			
	$DLSTM_*$	$BLSTM_{MC}$	$BLSTM_{VD}$	$BLSTM_{BBB}$
Batch size	216	216	216	32
Truncate sequence	100	100	100	128
Sequence size	100	100	100	64
Max epochs	100	100	100	200
LR	1e-2	1e-2	1e-2	1e-2
LR decay (per epoch)	1%	1%	1%	1%
Weight decay	1e-5	1e-5	–	–
Dropout (keep prob)	0.7	0.2	–	–
Optimizer	Adam	Adam	Adam	Adam

Original Dataset - 6 actions

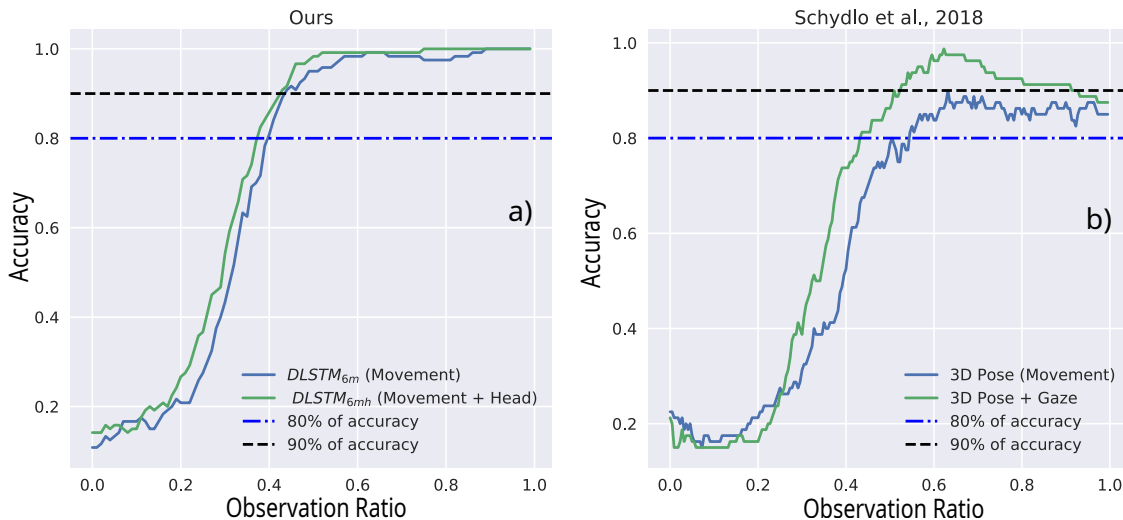


Figure 8: Results for deterministic models. In (a), the chart presents the accuracy of our model when using Movement and Movement+Head information. In (b), the chart presents the accuracy obtained by [17] when using pose and pose+gaze (the plotted points were provided by the authors)

charts illustrate how the model that uses only movement ($DLSTM_{12m}$) made a mistake in its anticipation. This mistake can be caused by overconfidence of the model when anticipating ambiguous actions. Other models, those ones which use part/complete context information, anticipated the action correctly. Notice that the model with full context (*head + object*), anticipated the action after observing only 2% of the data sequence (2 frames in its respective video).

Another interesting result is that the models confused those classes we supposed they would. After analyzing the videos, one can notice that action *pick right* has similar movement to *place right*, *give right* and *receive right*, and similar gaze to *place right*. Thus, $DLSTM_{12m}$ *pick right* mistook for *place right* and $DLSTM_{12m}$ was not certain about *pick right* and *receive right*. These characteristics appear in almost all predictions.

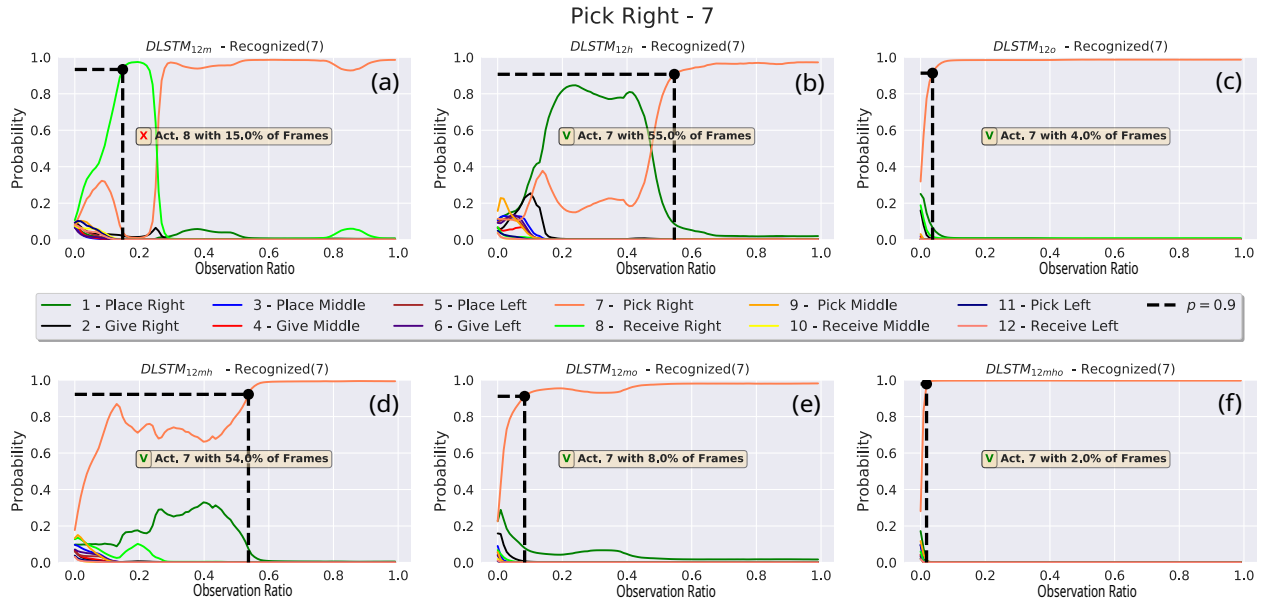


Figure 9: Evolution of sample of a *pick right* action for the six deterministic models.

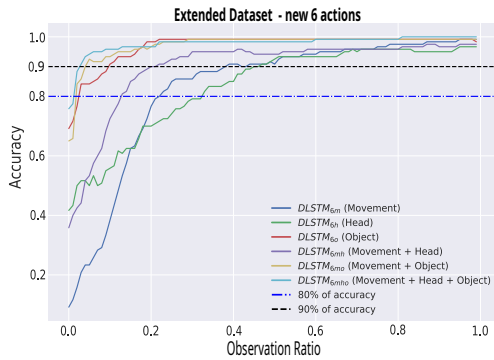


Figure 10: Results for deterministic models in the extended dataset only for the 6 new actions.

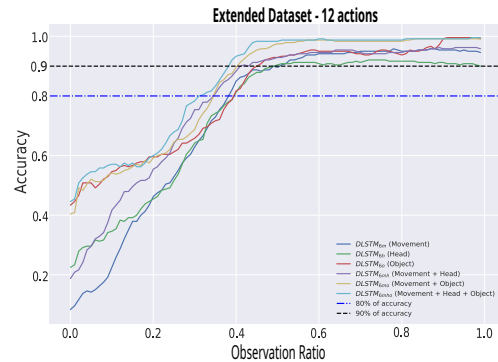


Figure 11: Results for deterministic models in the extended dataset (12 actions). Each experiment is the same model trained with different input data.

In order to highlight the trade-off between threshold and anticipation accuracy, the chart in Figure 12 presents the variation of anticipation accuracy and the percentage of observations w.r.t threshold (p). In the chart, we see that when $p = 0.9$, $DLSTM_{12mho}$ can anticipate correctly 95.42% of actions by using on average 19% of the video sequence. As usually, each action in Acticipate dataset has 79 images, this 19%

in observation ratio corresponds to an average of 15 frames of a video. On the other hand, by aiming the minimum number of observation, with $p = 0.8$, the model would anticipate correctly 92.08% of actions by using on average 18% of observation (14 frames).

With $p = 0.9$, function g (Equation(4)) is not able to consider overconfidence in the model prediction, which may generate many false-positives. As dis-

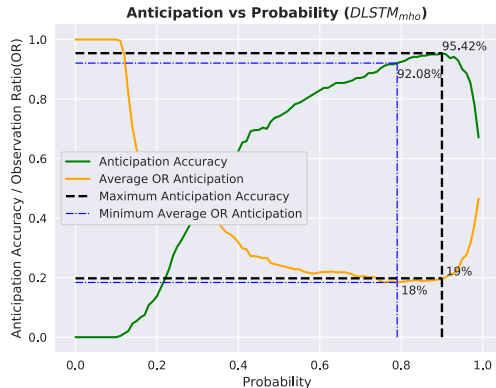


Figure 12: Variation of anticipation accuracy and average observation ratio w.r.t probability threshold.

cussed in Section 4, a possible solution to reduce the number of false-positives is to force the model to wait for more z observations to reaffirm its prediction. The problem with this approach is that z is a new parameter that can harm the anticipation, and must be chosen carefully. Figure 13 illustrates how anticipation accuracy ($p = 0.9$) and average observation ratio vary w.r.t z , where z is the additional observation ratio after anticipation. The best anticipation accuracy (97.02%) is achieved when $z = 0.18$. In other words, the model needs to wait on average for more 18% of observations in order to achieve an anticipation accuracy of 97.02%. Comparing with previous results, the gain of less than 2% in accuracy cost to the anticipation time an increase of more than the double of observations (passing from 19% to 43%). Furthermore, the minimum observation ratio necessary to anticipate any action is now 18%, even for action less ambiguous, such as those presented previously in Figure 3 and that used in Figure 9. Thus, besides the fact that the choice of z insert a new trade-off in the project (accuracy *vs* observation ratio), it does not provide an effective way to improve the action anticipation task.

8.2. Stochastic models

The results of the Bayesian models ($LSTM_{MC}$, $BLSTM_{VD}$ and $BLSTM_{BB}$) will be compared to $DLSTM_{12mho}$, our best deterministic model for the

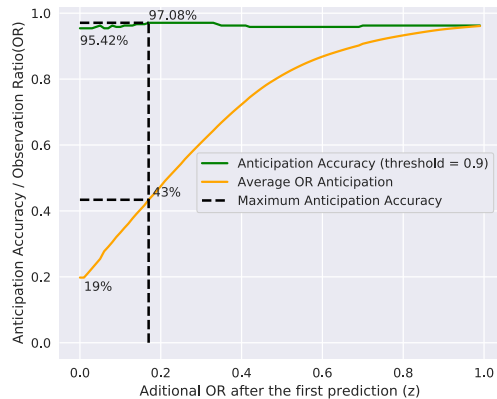


Figure 13: Variation of anticipation accuracy and average observation ratio w.r.t additional observation ratio after anticipation. If in time t the max probability exceeds the 0.9, the model must wait for more z observations in order to conform its prediction.

extended dataset. During prediction time, we fed each Bayesian model 20 times with the same observation \mathbf{x}_t , which corresponds to a MC sampling with $S = 20$. Next, by applying Equation (20) over the S predictions, we measured the epistemic uncertainty of each model prediction with respect to the observation \mathbf{x}_t . Then, we can use the Equation (28) to anticipate the action or not.

The Bayesian models also recognized all actions in the extended dataset. Furthermore, they achieved better results in anticipation accuracy than $DLSTM_{12mho}$, even if it waits for a observation ratio of $z = 0.18$. By applying the same procedure in Figure 12, we could choose a threshold value to be used in each model. Therefore, for each model, the anticipation threshold was chosen by analyzing the variation of anticipation accuracy and the average observation time w.r.t the uncertainty value. Figure 14 shows this comparison for $BLSTM_{MC}$.

Table 3 compares the results of the Bayesian models with our best deterministic model ($DLSTM_{12mho}$). Note that $BLSTM_{MC}$ achieves the best accuracy in anticipation task (98.75%) using the uncertainty threshold $u = 0.5$. However, $BLSTM_{VD}$ achieved 98.33% of anticipation accuracy and with $u = 0.3$

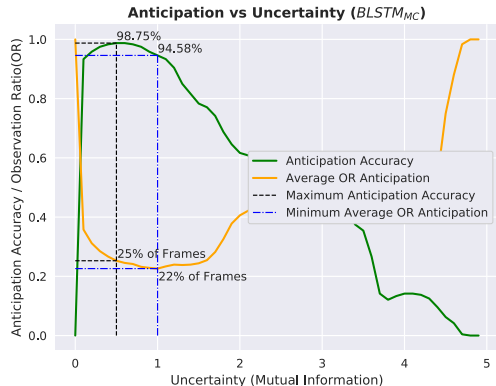


Figure 14: Variation of anticipation accuracy and average observation ratio w.r.t uncertainty threshold for MC dropout model

$BLSTM_{BBB}$ achieves 97.08%.

Considering the minimum number of observations necessary for good anticipation accuracy, $DLSTM_{12mho}$ gives the best result. On average, it needs to receive 18% of observations to achieve an anticipation accuracy of 92.08%. However, even though it needs fewer observations, it suffers a reduction of anticipation accuracy from 95.42% with $p = 0.9$ to 92.08% with $p = 0.79$. In summary, the best model achieved 98.75% after observing on average 25% of the action ($BLSTM_{MC}$). An increase of 6.67% in accuracy with a cost of only 7% in extra observations. Much better than using z in the deterministic model, where an increase of less than 2% costs 24% on extra observations. Besides, we do not need to choose more than one hyperparameter, only the uncertainty threshold u .

8.3. Discussions

As we already mentioned in the previous sections, for human-machine interaction, the model must not only have a short anticipation time but also be accurate in its prediction. For $BLSTM_{MC}$, it needs 25% of observations to achieve its best prediction value, which indeed is not a high value. For instance, in a system based on images sampled at 30Hz (ordinary cameras), an action that lasts 2 seconds would be anticipated by such a model after elapsed on average

0.5s from its first frame. In other words, it might anticipate action after the system observes on average 15 frames. Therefore, once the model can be considered accurate in its prediction, the system has about 1.5s to make a right decision.

As expected, our Bayesian models provided better results than deterministic ones with a small cost in additional observations. The overconfidence in model prediction decreases when waiting for more observations. However, as we could see, for deterministic models this is a new parameter to be chosen (z) and did not provide satisfactory results. On the other hand, by using uncertainty as threshold we have only one parameter to be chosen, and the model is able to achieve better results in accuracy with a small cost in observation ratio. These results support our last hypothesis that: uncertainty is a more reliable an effective threshold to anticipate action than probabilities are.

In our opinion, the MC dropout [37, 44] and variational dropout [38] were the best models implemented in this work. Once dropout and local reparametrization can provide a different sample for each observation, a mini-batch with S observations correspond to a MC sampling of size S , which helps model posterior distribution inference. In addition, for prediction, we only need to create a mini-batch of size S , repeating the same observation, that favors parallel prediction in GPUs. On the other hand, the reparametrization trick does not take advantage of the mini-batch to make samples. Every observation in the mini-batch uses the same sampled weight.

In consequence, in our experience, BBB models train slower than Bayesian dropout approaches, and, during prediction, it needs to run the model S times with the same observation, which does not allow to parallelize the prediction in GPUs. However, it seems that a significant advantage of BBB is the possibility of pruning the model by analyzing each parameter. As they are gaussian distributions, the relation mean-variance can indicate if a parameter is required or may be discarded [34, 36].

Finally, we could see that the proposed model outperformed our baseline [17] even using less accurate information (2D vs 3D pose and head joints vs eye gaze). The results supported the raised hy-

Table 3: Results of stochastic models and the best deterministic model.

Model	Parameter	Anticipation Accuracy	Average Observation Ratio
$DLSTM_{12mho}$	$p = 0.9 / z = 0.0$	95.42%	19%
$DLSTM_{12mho}$	$p = 0.79 / z = 0.0$	92.08%	18%
$DLSTM_{12mho}$	$p = 0.9 / z = 0.18$	97.08%	43%
$BLSTM_{MC}$	$u = 0.5$	98.75%	25%
$BLSTM_{MC}$	$u = 1.5$	94.58%	22%
$BLSTM_{VD}$	$u = 0.5$	98.33%	26%
$BLSTM_{VD}$	$u = 1.5$	85.42%	20%
$BLSTM_{BBB}$	$u = 0.3$	97.08%	25%
$BLSTM_{BBB}$	$u = 1.3$	93.33%	20%

potheses and showed how the uncertainty provided by Bayesian models is vital for action anticipation. Even though the presented results were acquired in a small collaborative dataset, our proposal can be used in other datasets. In this sense, it is necessary to analyze the possible sources of context for each class and adapt our embedding layer to represent all the context data.

9. Conclusions and Future Works

Machines need the capacity of anticipating actions to achieve effective interaction with humans. As such, the problem of action anticipation is drawing substantial research attention in recent years. Although the problem has been explored by many works, they do not provide a concise explanation about the importance of context to anticipate actions and do not discuss how to handle the problem of the uncertainty inherent of this kind of task.

We propose a stochastic (Bayesian) LSTM architecture that provides an uncertainty-based decision-making criterion. By selecting the action that minimizes the uncertainty, our model improves the action anticipation performance with respect to the conventional class-likelihood maximization (i.e. deterministic model).

Considering arm motion as the main source of information for action anticipation, we evaluate the influence of two additional (contextual) sources of information in the Acticipate dataset: gaze and object

attributes. When considering all sources of information in our stochastic LSTM, we achieved 100% of average accuracy in the action recognition task and 98.78% of average accuracy in the action anticipation task, outperforming previous results. Thus, our model serves both action recognition and anticipation purposes, while needing only 25% of the observations, on average, to anticipate each action. The results also show the clearly importance of context for the anticipation task, once the actions that depend on the eye gaze information or the object position had an impressive improvement on their anticipation time with respect to [17]. For instance, actions that depends exclusively on the object information are anticipated precociously, some of them with only two observations.

Our work extends the current state-of-the-art and results in action anticipation, for small collaborative datasets. In addition, our proposal of using context to improve the classification probability and the uncertainty as the decision-making criterion can be used in any other probabilistic model.

As future work, we aim to increase the complexity of the collaborative setup by adding more objects to each action, and design a collaborative scenario where the performed actions depend on more than one object.

Acknowledgments

This study was financed in part by the Coordenao de Aperfeioamento de Pessoal de Nvel Superior - Brasil (CAPES), PDSE/Process n 88881.188840/2018-01, Finance Code 001.

Bibliography

References

- [1] N. F. Duarte, M. Raković, J. Tasevski, M. I. Coco, A. Billard, J. Santos-Victor, Action anticipation: reading the intentions of humans and robots, *IEEE Robotics and Automation Letters* 3 (4) (2018) 4132–4139. doi:10.1109/LRA.2018.2861569.
- [2] Y. Kong, Y. Fu, Human action recognition and prediction: A survey, arXiv preprint arXiv:1806.11230.
- [3] K. He, X. Zhang, S. Ren, J. Sun, Deep residual learning for image recognition, in: *Proceedings of the IEEE conference on computer vision and pattern recognition*, 2016, pp. 770–778. doi:10.1109/CVPR.2016.90.
- [4] A. Krizhevsky, I. Sutskever, G. E. Hinton, Imagenet classification with deep convolutional neural networks, in: *Advances in neural information processing systems*, 2012, pp. 1097–1105. doi:10.1145/3065386.
- [5] K. Simonyan, A. Zisserman, Very deep convolutional networks for large-scale image recognition, arXiv preprint arXiv:1409.1556.
- [6] J. Devlin, M.-W. Chang, K. Lee, K. Toutanova, Bert: Pre-training of deep bidirectional transformers for language understanding, in: *Proceedings of the 2019 Conference of the North American Chapter of the Association for Computational Linguistics: Human Language Technologies, Volume 1 (Long and Short Papers)*, 2019, pp. 4171–4186. doi:10.18653/v1/N19-1423.
- [7] A. Vaswani, N. Shazeer, N. Parmar, J. Uszkor-eit, L. Jones, A. N. Gomez, L. Kaiser, I. Polosukhin, Attention is all you need, in: *Advances in neural information processing systems*, 2017, pp. 5998–6008.
- [8] A. Karpathy, G. Toderici, S. Shetty, T. Leung, R. Sukthankar, L. Fei-Fei, Large-scale video classification with convolutional neural networks, in: *Proceedings of the IEEE conference on Computer Vision and Pattern Recognition*, 2014, pp. 1725–1732. doi:10.1109/cvpr.2014.223.
- [9] K. Simonyan, A. Zisserman, Two-stream convolutional networks for action recognition in videos, in: *Advances in neural information processing systems*, 2014, pp. 568–576.
- [10] J. Carreira, A. Zisserman, Quo vadis, action recognition? a new model and the kinetics dataset, in: *proceedings of the IEEE Conference on Computer Vision and Pattern Recognition*, 2017, pp. 6299–6308. doi:10.1109/cvpr.2017.502.
- [11] H. Bilen, B. Fernando, E. Gavves, A. Vedaldi, Action recognition with dynamic image networks, *IEEE transactions on pattern analysis and machine intelligence* 40 (12) (2017) 2799–2813. doi:10.1109/tpami.2017.2769085.
- [12] C. Rodriguez, B. Fernando, H. Li, Action anticipation by predicting future dynamic images, in: *Proceedings of the European Conference on Computer Vision (ECCV)*, 2018, pp. 0–0. doi:10.1007/978-3-030-11015-4_10.
- [13] V. Choutas, P. Weinzaepfel, J. Revaud, C. Schmid, Potion: Pose motion representation for action recognition, in: *Proceedings of the IEEE Conference on Computer Vision and Pattern Recognition*, 2018, pp. 7024–7033. doi:10.1109/cvpr.2018.00734.
- [14] H. Kwon, Y. Kim, J. S. Lee, M. Cho, First person action recognition via two-stream convnet with long-term fusion pooling, *Pattern Recognition Letters* 112 (2018) 161–167. doi:10.1016/j.patrec.2018.07.011.

- [15] F. Baradel, N. Neverova, C. Wolf, J. Mille, G. Mori, Object level visual reasoning in videos, in: Proceedings of the European Conference on Computer Vision (ECCV), 2018, pp. 105–121.
- [16] Y. LeCun, Y. Bengio, et al., Convolutional networks for images, speech, and time series, The handbook of brain theory and neural networks 3361 (10) (1995) 1995.
- [17] P. Schydlo, M. Rakovic, L. Jamone, J. Santos-Victor, Anticipation in human-robot cooperation: A recurrent neural network approach for multiple action sequences prediction, in: 2018 IEEE International Conference on Robotics and Automation (ICRA), IEEE, 2018, pp. 1–6. doi: [10.1109/ICRA.2018.8460924](https://doi.org/10.1109/ICRA.2018.8460924).
- [18] A. K. Dey, G. D. Abowd, Towards a Better Understanding of Context and Context-Awareness, Computing Systems 40 (3) (1999) 304–307. doi: [10.1007/3-540-48157-5_29](https://doi.org/10.1007/3-540-48157-5_29).
- [19] H. Wang, J. Feng, Delving into 3d action anticipation from streaming videos, arXiv preprint arXiv:1906.06521.
- [20] F. Pirri, L. Mauro, E. Alati, V. Ntouskos, M. Izadpanahkakhk, E. Omrani, Anticipation and next action forecasting in video: an end-to-end model with memory, arXiv preprint arXiv:1901.03728.
- [21] S. Agethen, H.-C. Lee, W. H. Hsu, Anticipation of human actions with pose-based fine-grained representations, in: Proceedings of the IEEE Conference on Computer Vision and Pattern Recognition Workshops, 2019, pp. 0–0.
- [22] Y. Shi, B. Fernando, R. Hartley, Action anticipation with rbf kernelized feature mapping rnn, in: Proceedings of the European Conference on Computer Vision (ECCV), 2018, pp. 301–317. doi: [10.1007/978-3-030-01249-6_19](https://doi.org/10.1007/978-3-030-01249-6_19).
- [23] J.-F. Hu, W.-S. Zheng, L. Ma, G. Wang, J.-H. Lai, J. Zhang, Early action prediction by soft regression, IEEE transactions on pattern analysis and machine intelligence doi: [10.1109/TPAMI.2018.2863279](https://doi.org/10.1109/TPAMI.2018.2863279).
- [24] M. Sadegh Aliakbarian, F. Sadat Saleh, M. Salzmann, B. Fernando, L. Petersson, L. Andersson, Encouraging lstms to anticipate actions very early, in: Proceedings of the IEEE International Conference on Computer Vision, 2017, pp. 280–289. doi: [10.1109/iccv.2017.39](https://doi.org/10.1109/iccv.2017.39).
- [25] H. Bilen, B. Fernando, E. Gavves, A. Vedaldi, S. Gould, Dynamic image networks for action recognition, in: Proceedings of the IEEE Conference on Computer Vision and Pattern Recognition, 2016, pp. 3034–3042. doi: [10.1109/cvpr.2016.331](https://doi.org/10.1109/cvpr.2016.331).
- [26] V. Bloom, V. Argyriou, D. Makris, Linear latent low dimensional space for online early action recognition and prediction, Pattern Recognition 72 (2017) 532–547. doi: [10.1016/j.patcog.2017.07.003](https://doi.org/10.1016/j.patcog.2017.07.003).
- [27] D. Wang, Y. Yuan, Q. Wang, Early action prediction with generative adversarial networks, IEEE Access 7 (2019) 35795–35804. doi: [10.1109/ACCESS.2019.2904857](https://doi.org/10.1109/ACCESS.2019.2904857).
- [28] X. Wang, J.-F. Hu, J.-H. Lai, J. Zhang, W.-S. Zheng, Progressive teacher-student learning for early action prediction, in: Proceedings of the IEEE Conference on Computer Vision and Pattern Recognition, 2019, pp. 3556–3565.
- [29] Y. Ji, Y. Yang, X. Xu, H. T. Shen, One-shot learning based pattern transition map for action early recognition, Signal Processing 143 (2018) 364–370. doi: [10.1016/j.sigpro.2017.06.001](https://doi.org/10.1016/j.sigpro.2017.06.001).
- [30] P. Felsen, P. Agrawal, J. Malik, What will happen next? forecasting player moves in sports videos, in: Proceedings of the IEEE International Conference on Computer Vision, 2017, pp. 3342–3351. doi: [10.1109/iccv.2017.362](https://doi.org/10.1109/iccv.2017.362).
- [31] L. Neumann, A. Zisserman, A. Vedaldi, Future event prediction: If and when, in: Proceedings

- of the IEEE Conference on Computer Vision and Pattern Recognition Workshops, 2019, pp. 0–0.
- [32] M. Kassner, W. Patera, A. Bulling, Pupil: an open source platform for pervasive eye tracking and mobile gaze-based interaction, in: Proceedings of the 2014 ACM international joint conference on pervasive and ubiquitous computing: Adjunct publication, ACM, 2014, pp. 1151–1160.
- [33] D. M. Blei, A. Kucukelbir, J. D. McAuliffe, Variational inference: A review for statisticians, *Journal of the American Statistical Association* 112 (518) (2017) 859–877. doi:10.1080/01621459.2017.1285773.
- [34] A. Graves, Practical variational inference for neural networks, in: Advances in neural information processing systems, 2011, pp. 2348–2356.
- [35] D. P. Kingma, M. Welling, Auto-encoding variational bayes, arXiv preprint arXiv:1312.6114.
- [36] C. Blundell, J. Cornebise, K. Kavukcuoglu, D. Wierstra, Weight uncertainty in neural network, in: International Conference on Machine Learning, 2015, pp. 1613–1622.
- [37] Y. Gal, Z. Ghahramani, Dropout as a bayesian approximation, in: 33rd International Conference on Machine Learning, ICML 2016, Vol. 3, 2016, pp. 1661–1680.
- [38] D. P. Kingma, T. Salimans, M. Welling, Variational dropout and the local reparameterization trick, in: Advances in Neural Information Processing Systems, 2015, pp. 2575–2583.
- [39] A. Kendall, Y. Gal, What uncertainties do we need in bayesian deep learning for computer vision?, in: Advances in neural information processing systems, 2017, pp. 5574–5584.
- [40] D. Hafner, D. Tran, A. Irpan, T. Lillicrap, J. Davidson, Reliable uncertainty estimates in deep neural networks using noise contrastive priors, arXiv preprint arXiv:1807.09289.
- [41] Y. Gal, Uncertainty in deep learning, Ph.D. thesis, PhD thesis, University of Cambridge (2016).
- [42] Z. Cao, G. Hidalgo Martinez, T. Simon, S. Wei, Y. A. Sheikh, Openpose: Realtime multi-person 2d pose estimation using part affinity fields, *IEEE Transactions on Pattern Analysis and Machine Intelligence* (2019) 1–1 doi:10.1109/TPAMI.2019.2929257.
- [43] S. Hochreiter, J. Schmidhuber, Long short-term memory, *Neural computation* 9 (8) (1997) 1735–1780. doi:10.1162/neco.1997.9.8.1735.
- [44] Y. Gal, Z. Ghahramani, A theoretically grounded application of dropout in recurrent neural networks, in: Advances in neural information processing systems, 2016, pp. 1019–1027.